Atmos. Chem. Phys. Discuss., 6, 7623–7656, 2006
www.atmos-chem-phys-discuss.net/6/7623/2006/

Atmospheric Chemistry and Physics Discussions

Consecutive reactions of aromatic–OH adducts with NO, NO_2 and O_2: benzene, toluene, m- and p-xylene, hexamethylbenzene, phenol, m-cresol and aniline

R. Koch[1,2], **R. Knispel**[1], **M. Elend**[1], **M. Siese**[1,2], **and C. Zetzsch**[1,2]

[1]Fraunhofer-Institute of Toxicology and Experimental Medicine, Hannover, Germany
[2]Atmospheric Chemistry Research Laboratory, University of Bayreuth, Germany

Received: 26 June 2006 – Accepted: 26 July 2006 – Published: 9 August 2006

Correspondence to: C. Zetzsch (cornelius.zetzsch@uni-bayreuth.de)

Abstract

Consecutive reactions of adducts, resulting from OH radicals and aromatics, with the tropospheric scavenger molecules O_2, NO and NO_2 have been studied for benzene, toluene, m- and p-xylene, hexamethylbenzene, phenol, m-cresol and aniline by observing decays of OH at temperatures where the thermal back-decomposition to OH is faster than $3\,s^{-1}$, typically between 300 and 340 K. The experimental technique was resonance fluorescence with flash photolysis of water as source of OH. Biexponential decays were observed in the presence of either O_2 or NO, and triexponential decays were obtained in the presence of NO_2. The kinetic analysis was performed by fitting the relevant rate constants of the reaction mechanism to whole sets of decays obtained at various concentrations of aromatic and scavenger. In the case of hexamethylbenzene, the biexponential decays suggest the existence of the ipso-adduct, and the slightly higher necessary temperatures show that it is even more stable.

In addition, smog chamber experiments at O_2 concentrations from atmospheric composition down to well below 100 ppm have been carried out for benzene, toluene and p-xylene. The drop of the effective rate constant of removal by OH occurs at reasonable O_2 levels, given the FP/RF results. Comparison of the adduct reactivities shows for all aromatics of this study that the reaction with O_2 predominates over that with NO_2 under all tropospheric conditions, and that a reaction with NO may only occur after the reaction with O_2.

1 Introduction

Aromatic hydrocarbons are a major class of anthropogenic compounds emitted to the troposphere. Despite emission control measures, they still account for 20 to 30% of the non-methane hydrocarbons in urban air (see Chapter I of the monograph by Calvert et al. (2002). As they react rapidly with OH radicals, they have a strong influence on urban air quality. Their high ozone creation potential is not yet fully understood and

justifies further work on their degradation mechanism (Jenkin et al., 2003; Bloss et al., 2004). This paper summarises our work on the consecutive steps of OH-initiated degradation of aromatic compounds in the presence of the typical atmospheric radical scavengers NO, NO_2 and O_2.

The hydroxyl initiated degradation of aromatics and the respective reaction mechanisms have been studied using various experimental techniques (see reviews by Atkinson, 1989, 1994; and Atkinson and Arey, 2004). The kinetics attributed to the formation of the addition complex, the equilibrium between the adduct, aromatic–OH, and the educts, and the abstraction of an H atom from the aromatic ring or from a substituent have been observed over a wide range of temperature and pressure. They have been studied in our laboratory as well (Wahner and Zetzsch, 1983; Rinke and Zetzsch, 1984; Witte et al., 1986) and are fairly well understood.

In tropospheric chemistry, however, the competition of the consecutive reactions of the adducts with scavenger molecules, such as NO, NO_2, O_2 and other atmospheric constituents, the possible reaction pathways and resulting product distributions are of major interest. These aspects have been studied by laser photolysis/laser absorption and laser photolysis/UV absorption by Zellner et al. (1985); Bohn and Zetzsch (1999); Bohn (2001); Johnson et al. (2002, 2005); Raoult et al. (2004) and Grebenkin and Krasnoperov (2004), by discharge-flow/laser induced fluorescence (Goumri et al., 1990); in flash photolysis/resonance fluorescence studies by Perry et al. (1977), Zetzsch et al. (1990) and Knispel et al. (1990) for benzene, toluene and phenol; and in product studies by Atkinson et al. (1989), Atkinson and Aschmann (1994), Bethel et al. (2000), Berndt and Böge (2001a, 2001b, 2006) and Volkamer et al. (2002) and Klotz et al. (2002) for benzene, toluene, o- and p-xylene, hexamethylbenzene (HMB) and 1,2,3- and 1,2,4-trimethylbenzene.

In the following, we present a kinetic study of the consecutive reactions of aromatic–OH adducts in the presence of variable amounts of either NO, NO_2 or O_2. Most of the results on benzene, toluene, p-xylene, phenol and m-cresol were obtained using the VUV flash photolysis/resonance fluorescence (FP/RF) technique, introduced by

Stuhl and Niki (1972). The data on benzene, toluene and phenol have been reported previously (Knispel et al., 1990), but some of those measurements (benzene–OH and toluene–OH + O_2 and phenol–OH + NO_2) have been re-evaluated using improved software-tools. The data on p-xylene, m-xylene, m-cresol and aniline have been briefly reported by Koch et al. (1994) and Zetzsch et al. (1997) and are described in more detail in the present study. The adduct reaction was furthermore examined by a smog chamber technique in N_2 with continuous addition of O_2 (Elend and Zetzsch, 1992) for benzene, toluene and p-xylene.

2 Methods

2.1 Flash photolysis/resonance fluorescence setup

The basic components are a flash lamp, a resonance lamp and a fluorescence detector mounted at right angles to each other. In the following description, emphasis is on improvements of both the set-up and evaluation procedure over what has been used by Wahner and Zetzsch (1983) and Witte et al. (1986).

2.1.1 Data acquisition and hardware

A multichannel scaler board (EG&G Ortec, model ACE MCS) with 4096 channels is used on a PC, which also controls the triggering of the flash lamp and the flows, pressures and temperatures of the experiment. The PC is equipped with a multi-I/O card (Meilhaus PC30, 16x 12-bit A/D, 4x D/A, 24 bit I/O) supplemented by a card with 8 D/A converters (Bockstaller, PC8408). Since multiplexing the temperature signals at the sensor level proved to be unreliable, separate converter modules (Analog Devices, 5B34) for each Pt100 resistor were multiplexed at the 5-V level (Analog Devices, 5B02).

2.1.2 Software running the experiment

A TurboPascal program was developed featuring: low-level control of the hardware; calculation of the settings necessary for intended concentrations in the cell and *vice versa*, applying calibration data for each device as well as Antoine constants for the partial pressure in the saturators; graphical presentation of the decay while it is summed up, together with a preliminary exponential fit; a user interface allowing the operator to change all the settings interactively; a batch language with one command for each menu entry of the user interface and directives for calling subroutines, i.e. other batch files, for the convenient programming of measurement tasks. Batch processing can be interrupted at any level of nested subroutines and can be resumed after a problem has been fixed or continued with the current batch file adapted to the latest findings.

2.1.3 Precautions for semivolatile compounds and a wider temperature range

To avoid condensation of low-reactivity, low-vapour-pressure compounds, the glass tubing from the thermostated saturator to the cell was heated up to and including the needle valve where the gas expands from atmospheric to cell pressure. The black anodized surface of the cell and the flanges has been removed where it prevented gas-tight contact to o-rings, lowering the leakage rate of the cell to 0.25 mbar ml/min, 0.2 ppm of the typical buffer-gas flow. Viton o-rings, degassing reactive compounds at high temperatures, were replaced by odorless silicone-rubber o-rings (Busak + Luyken) leading to longer lifetimes of OH.

2.1.4 Modifications of the flash lamp

A quartz lens (Heraeus, Suprasil, f_{vis}=50 mm) mounted 9 cm from the spark focuses the VUV flash to a point well before the MgF_2 entrance window. The aim was not to increase the radical concentration (see below) but to widen the beam inside the cell: The volume, where H_2O is photolysed, is wider than the field of view of the multiplier

so that the influence of diffusion and the slow flow through the cell on the decay rates can be neglected during the first second after the flash at the typical total pressure of 130 mbar. A cuvette may be placed at the intermediate focus in order to filter the VUV flash-light. This option was used in the case of p-xylene where an interfering fluorescence signal lasting several milliseconds after the flash was diminished by a 2-cm preabsorbing layer of p-xylene vapour. Most experiments were performed using a flash energy of 2 J, a few experiments (on m-xylene) were performed using an excimer laser (EMG102, Lambda Physics) at 193 nm with an energy fluence of 10 mJ/cm^2 instead of the flash lamp, photolysing N_2O and converting the resulting $O(^1D)$ to OH by the rapid reaction with H_2O. The experiments with HMB were performed with a flash lamp of 0.5 J, omitting the defocusing quartz lens.

2.1.5 Measures to increase the signal intensity

The shape of the glass tube of the resonance lamp was modified to widen just above and below the $\lambda/4$ resonator, which has been silver plated for reducing losses of microwave power. The spreading plasma is concentrated towards the point of efficient light collection by increasing the pressure to several mbar, and the aperture of the lamp is approximately doubled. The four collimating and focusing lenses, two for the lamp and multiplier each, are antireflection-coated for 300 nm. The interference filter towards the multiplier has been replaced by one with slightly wider transmission curve (FWHM, 9 nm) but considerably higher peak transmission (47% at 309 nm, Anders, Nabburg). The total effect was an increase of signal intensity from 40 to 190×10^3 counts/s. Although the background increased even more (from 5 to 40), the signal-to-noise ratio improved by a factor of 1.7, allowing us to decrease the concentration of water from 3 to 2×10^{15} cm^{-3}, which decreases the signal to 160×10^3 counts/s. The initial OH concentration is now well below 10^{10} cm^{-3} estimated by comparing signal intensities (corrected for fluorescence quenching by H_2O): By titrating 6×10^{11} cm^{-3} NO_2 with excess H atoms generated by 193-nm photolysis of NH_3, OH is visible over 6 orders of magnitude. Thus, build-up of reaction products, depletion of aromatics and

radical–radical-reactions are all negligible.

2.1.6 Measures to stabilize the signal

A microwave generator (Muegge, Reichelsheim, MW-GPRYJ1511-300-01, 2.45 GHz, 300 W) with a switching-mode power supply for the magnetron eliminated 100-Hz ripple, and intermittent flicker was remedied by supplying the microwave power, typically 200 W, to the lamp via a circulator (Philips, Type 2722 163 02071), absorbing the reflected power. The influence of possibly remaining low-frequency noise and drift is reduced by determining the background as close as possible to where it is needed, i.e. at the end of the decay (recorded up to 5 s). Typically, 50 to 150 scans are accumulated for a decay curve. If necessary, repeated recordings are coadded after visual inspection. The first one or two channels have to be omitted due to an afterglow of the flash lamp, lasting about 1.5 milliseconds.

2.1.7 Data reduction and evaluation

During the slow decay into the noise of the already subtracted background, binning the photons into the millisecond time slots of the multichannel scaler is neither necessary nor appropriate. The irrelevant high-frequency noise that is characteristic of the photon-counting technique would obscure both, low-frequency noise and signal. Even worse, in a semi-log plot, where negative values have to be omitted and small values are largely expanded, the highest density of data points would appear above the mean value. Therefore, the data is rebinned in a manner appropriate for decay curves that are sums of exponentials: The interval width is doubled whenever the elapsed time is 12 times the actual width, i.e. every sixth interval. By this procedure, the original 4096 data points are compressed into 62 values which are roughly equidistant on a logarithmic time scale. It has been tested by evaluation of synthetic, noisy, biexponential decays that even much coarser binning would not lead to systematic deviations. This enables us to demonstrate a dynamic range of three orders-of-magnitude in a clear plot. It

should be noted that, for the fitting procedure, it is not the plotted function values of modelled decay curves that are compared to the coarsely binned data, but the integrals of the curves over the very same time intervals.

Reaction mechanism and kinetic analysis (FP/RF): The following reaction mechanism, where A is the aromatic, AOH the adduct and S the scavenger, is considered in the resonance fluorescence experiments:

$$OH + A \leftrightarrow AOH \quad (1/-1)$$

$$OH + A \rightarrow \quad (2)$$

$$OH + S \rightarrow \quad (3)$$

$$OH \rightarrow \quad (4)$$

$$AOH \rightarrow \quad (5)$$

$$AOH + S \rightarrow \quad (6)$$

The differential equation governing the reversible formation of an adduct, AOH, with loss processes on either side of the equilibrium is given as Eq. (I):

$$\frac{d}{dt}[OH] = -a[OH] + b[AOH] \quad (I)$$
$$\frac{d}{dt}[AOH] = c[OH] - d[AOH]$$

The coefficients c and b are the rate constants for adduct formation and back-decomposition, Reaction (1/–1), while a and d additionally contain the irreversible loss processes, Reactions (2) to (6):

$a = k_4 + (k_1 + k_2)[A] + k_3[S]$, $b = k_{-1}c = k_1[A]$ and $d = k_1 + k_5 + k_6[S]$, where [A] and [S] are the aromatic and the scavenger concentration, respectively, and [AOH] is the concentration of the thermolabile adduct, aromatic–OH. Note that the formal Reaction (2),

which represents the part of *a–c* which is proportional to [A], contains the abstraction channel as well as the reaction of OH with possible impurities of the aromatic. Reaction (3) is used for NO or NO_2 as scavenger only, since O_2 has been tested to be pure enough not to decrease the lifetime of OH. Reaction (4) is called diffusion loss but also contains reactions of OH with background impurities of the cell as well as an offset error in [A]. Similarly, Reaction (5) may comprise a unimolecular isomerisation of the adduct as well as an offset error of the flow controllers employed for the scavenger or a background of O_2 from leaks.

The analytic solution of Eq. (I), already given by Wahner and Zetzsch (1983), is the sum of two exponential components $I \times e^{-t/\tau}$ for each of [OH](t) and [AOH](t) with common parameters τ_1^{-1} and τ_2^{-1}:

$$\tau_{1,2}^{-1} = \frac{a+d}{2} \pm \sqrt{\left(\frac{a+d}{2}\right)^2 - bc} \qquad \text{(IIa)}$$

The ratio of the amplitudes, I_1/I_2, for the OH part of the solution is given by

$$I_1/I_2 = \frac{(\tau_1^{-1} - d)^2}{bc} \qquad \text{(IIb)}$$

while for the adduct it is simply –1.

The coefficients *b* and *c* occur in Eq. (II) only as a product, see Appendix. This has no effect on the evaluation of the title reactions.

Note that while the dependence of τ_2^{-1} on the concentration of the scavenger may appear linear for a given data set, an evaluation according to $\tau_2^{-1} = k_5 + k_6[S]$ (implying the approximation $\tau_2^{-1} \approx d$) can be considerably in error, especially in the case of NO as scavenger, due to Reaction (3). The influence of k_3 on τ_2^{-1} becomes marginal as I_1/I_2 exceeds 100, but then, however, τ_2^{-1} is barely visible in decays of OH.

2.1.8 Fitting strategy

The two exponentials are fitted simultaneously, using as fit parameters either τ_1^{-1}, τ_2^{-1} and I_1/I_2; or *a*, *d* and *bc* (the former set can be converted into the latter by inverting Eqn. (II), starting with $\tau_1^{-1} + \tau_2^{-1}$ and $\tau_1^1 \tau_2^{-1}$). We call such fits "e-fits". Sets of biexponential decays obtained at various concentrations of aromatic and scavenger lead to sets of *a*, *d* and *bc,* varying linearly with the concentrations.

We took a further step (Koch, 1992): Sets of biexponential decays were analysed simultaneously by fitting the slopes (and diffusion offsets) of *a*, *d* and *bc*, see Appendix, directly to the data. The Levenberg-Marquardt algorithm (see Press et al., 1992) is employed in a comfortable Pascal program, that allows to (i) adjust the time ranges for fitting either the background or decaying parts, to (ii) e-fit decays in a batch with individual start parameters calculated from [A] and [S], and to (iii) select subsets of decays for k-fitting a bunch of model functions to them (in fact, the functions may be watched "dancing" around the data if the PC is not too fast). The result can be displayed on the screen as succession of residua; written to a protocol file as set of rate constants with their variances and covariances, and as table of exponential parameters to be compared to the results of e-fits; and written as time profiles to a spreadsheet to be plotted. All settings are saved for the next run of the program.

The benefit of this simultaneous fit (k-fit) is greatest for decays that are not distinctly biexponential, i.e., if τ_1^{-1} and τ_2^{-1} are separated by a factor of less than, say, 3. In these cases, the exponential parameters would have large mutual covariances, i.e., different sets of parameters would describe the decay almost equally well. The k-fit skips this shaky ground (see the Results section for an example). Another benefit is the ease of including proper weights (the number of scans divided by the modelled intensity including background integrated over each time interval) with the result of realistic statistical error limits of the rate constants obtained. Care has to be taken to ensure that the decays differ only in parameters included in the model. Changes in the strongly temperature-dependent back-decomposition, for example, are not treated

as such, since k_{-1} is a common fit parameter. Instead, other fit parameters would be influenced due to the covariances between them. On the other hand, the k-fit copes with an unintended variation of reactant concentration, which would be a problem for the classical two-step approach (analysis of e-fit results obtained at constant [R] and varied [S]).

In the presence of NO_2, its rapid reaction with H atoms originating from the photolysis of H_2O leads to an additional OH source-term and thus to a third exponential component in the decays (see Results section).

2.1.9 Chemicals

Deionized and bidestilled water is used. Aromatics, except benzene and toluene (Rathburn, >99.8%, glass distilled grade), are obtained from Aldrich (m- and p-xylene and HMB for analysis, >99% (GC), phenol redistilled, >99%, m-cresol, 99%, aniline, glass distilled grade, >99.5% (GC)) and are dispensed by the saturator method (Wahner and Zetzsch, 1983), usually from the liquid phase except benzene and HMB.

Since impurities are transported and concentrated by a slowly progressing solid-liquid phase-boundary, benzene had to be further purified by freeze-pump-thaw cycles, until k_{OH} becomes stable, before it is rapidly frozen for the last time. Concentrations of the aromatics were chosen, depending on their k_{OH}, for τ_1^{-1} to be between 100 and 200 s^{-1}, and it has been checked that photolysis is negligible by varying the flash energy between 1.6 and 5 J, without a considerable effect on decay rates.

All gases were obtained from Messer Griesheim. Oxygen (>99.998%) is used without further purification up to some 10^{17} cm^{-3}. For the lower concentrations, needed for the phenolics, mixtures of about 2000 vpm O_2 in He were produced using flow controllers and stored in a 2-l cylinder. Up to 5×10^{13} cm^{-3} NO is added from a 2000-vpm mixture with Ar (specified by the manufacturer to be within ±2%) and is purified from NO_2 impurities by a $FeSO_4\times7H_2O$ scrubber. As determined by H–to–OH conversion, the NO_2/NO ratio decreases from about 2×10^{-2} to below 10^{-4}. To prevent the forma-

tion of OH from peroxy radicals (the oxidation of background impurities may proceed with less O_2 than of the aromatics), the buffer gas, usually 130 mbar of Ar (>99.998%), is purified from traces of oxygen using Oxisorb (Messer Griesheim). Up to 7×10^{11} cm^{-3} NO_2 is added using permeation tubes (Vici Metronics) calibrated to ±2% by monitoring their loss of mass.

2.2 Smog chamber

The removal of the aromatic–OH adducts by O_2 is investigated in a smog chamber, described by Behnke et al. (1988), with 2450 l volume at 300 K in N_2 at atmospheric pressure at O_2 levels between about 50 ppm and 21%, as briefly reported by Elend and Zetzsch (1992). The N_2 gas, taken from liquid nitrogen (Messer Griesheim), was determined by GC-ECD analysis to contain less than 10 ppm O_2. Low levels of O_2 are reached in the smog chamber by flushing the O-ring seals with N_2 from outside. OH radicals are produced by photolysis of H_2O_2 using 7 medium-pressure arc lamps (Metallogen HMI, Osram, 1200 W). H_2O_2 (Peroxid-GmbH, >80%, stabilised) is kept constant at about 500 ppb by continuously adding 1 ppm/h from an impinger, containing 98 wt-% H_2O_2 and flushed continuously to keep H_2O_2 constant. Starting from different levels, O_2 is added continuously to the chamber and determined at 30-min intervals by GC/ECD analysis of 0.2-ml gas samples (Chrompack CP Sil 8 CB, 25 m, 0.32 mm inner diameter, 1.27 μm film thickness). The O_2 response is calibrated by chamber runs with exponential dilution, checked for stability against an electrochemical analyser (Oxanal, Gerhard GmbH, Blankenbach) before and after each chamber run.

The aromatics and the reference compounds (n-butane, tetramethylbutane, n-heptane and the inert perfluorohexane), initially 5–40 ppb each, are determined every 30 min from 20-ml gas samples using cryogenic trapping (Nolting et al., 1988) and GC/FID (Chrompack Al_2O_3 PLOT).

Peak areas are divided, sample per sample, by the area of the perfluorohexane peak to correct for dilution of the chamber content during the run. The remaining decrease is obviously consumption by OH, as the [OH] profiles obtained from the ref-

erence compounds agree with each other within 5%, if the k_{OH} values 1.10, 2.56 and 7.30×10^{-12} cm^3 s^{-1} are used for tetramethylbutane, n-butane and n-heptane, respectively, which are well-established in our laboratory (Behnke et al., 1988). These values meet the recommendations of Atkinson (1994) at 300 K. Using the average [OH](t), the apparent OH rate constant of the aromatic is then calculated as a function of time and plotted against [O_2].

3 Results

3.1 Aromatic–OH + O_2

At the high O_2 levels of 10^{17} cm^{-3} needed to observe any reaction with benzene–OH, part of the VUV is absorbed between entrance window and detection volume, adding to the gradient of $[OH]_{t=0}$ due to the divergence of the beam. It has been checked that, in the absence of benzene, [OH](t) does not depend on [O_2] except for its amplitude. Oxygen atoms and ozone are formed in concentrations estimated to be negligible.

For benzene–OH, the reaction rate constant with O_2 has been obtained at four temperatures in the range 299 to 354 K. In order to keep the slow exponential component at a detectable level with decreasing temperature, the rate of adduct formation ($\approx\tau_1^{-1}$) must be reduced with the rate of its thermal back-decomposition, thus limiting the range of variation of τ_2^{-1}. For this reason and due to the quenching of the resonance fluorescence by O_2, the absolute error is higher at 299 K, see Table 1. How the k-fit helps to include decays with $\tau_2^{-1}\approx\tau_1^{-1}$, becomes more obvious with the stronger signals in the case of m-cresol where 10^{15} cm^{-3} of O_2 are sufficient: Fig. 1 shows decays obtained at 334 K with curves representing the result of the k-fit. Note that the two steepest decays differ considerably and therefore contain information about the target reaction, but that the steepest one would be impossible to evaluate by an e-fit due to instability (see Methods section). Figure 2 shows the case of hexamethylbenzene, for which the temperature had to be raised by about 40 K compared to the other monoaromatics, indicating a higher stability of the ipso-adduct. Results on the eight aromatic compounds of this study are listed in Table 1.

Experiments had also been made with naphthalene (Koch and Zetzsch, 1994) at temperatures well above 370 K, where the OH-adduct starts to decompose on the FP/RF time-scale. These suffer, however, not only from low signal intensities due to quenching of the OH-fluorescence by O_2 but also from sticky reaction products, which increase the background reactivity of the cell and are photolysed by the flash to produce OH and other radicals (OH decays were observed with only He flowing through the cell). Recent measurements with a different flash lamp (10 instead of 50 nF capacitor, spectrum limited by the MgF_2 window instead of a Suprasil lens for a more effective photolysis of water compared to organics) and further improved detection limit (polished microwave resonator, He instead of Ar in the lamp) yielded apparent O_2 reactivities well below the former result of 1.1×10^{-16} cm^3 s^{-1} and show a marked dependence on H_2O concentration, i.e. radical and product level. Thus, k(naphthalene–OH + O_2) at 400 K may well be less than 10^{-17} cm^3 s^{-1}, in accordance with the negative temperature dependence observed in experiments at 336 and 298 K (Koch and Zetzsch, 1994) employing cycling of radicals (Koch et al., 1994 and 1997).

3.2 Aromatic–OH + NO_2

In the presence of NO_2, the rapid reaction of H atoms (originating from the photolysis of H_2O) with NO_2 generates additional OH and leads to a third exponential component. The model is supplemented by the respective rate constant, 1.3×10^{-10} cm^3 s^{-1} (Wagner and Welzbacher, 1976; Michael et al., 1979), plus an H-atom diffusion term, and the triexponential solution is used in the analysis. Note that in the case of NO_2 as scavenger, coefficient a contains a term proportional to [NO_2]. For the respective rate constant (OH + NO_2 + M), measurements in the absence of aromatic yielded 2.4×10^{-12} cm^3 s^{-1} at 133 mbar in Ar at 319 K, in good agreement with the literature (Paraskevopoulos and Singleton, 1988).

For most aromatics, the model matches the shape of the observed OH time profiles quite well, see for example Fig. 2 in our previous paper (Knispel et al., 1990). In the case of p-xylene, shown in Fig. 3, the deviations during the first 30 milliseconds indicate a higher initial H-atom concentration. It appears that the VUV photolysis of p-xylene leads to the formation of H atoms. At t>60 ms, however, the [OH]/[AOH] ratios, which influence the effective loss rate depending on losses on both sides of the equilibrium, are thought not to be distorted by the fast H–to–OH conversion, and that part of the decays is used for a k-fit (with the parameters describing the scavenger-free system held fixed). As can be seen in Fig. 3, the model adequately describes the [NO_2]-dependence of τ_2^{-1}. The results on the six aromatic compounds studied with NO_2 are listed in Table 1.

3.3 Behaviour of the adducts in the presence of NO

For the case of NO as scavenger, the rate constant of the interfering reaction with OH is determined in the absence of aromatics to be 0.95×10^{-12} cm^3 s^{-1} at 320–343 K with 133 mbar of Ar as third body, in good agreement with literature data of Anastasi and Smith (1979) and reviewed by Paraskevopoulos and Singleton (1988). This loss of OH increases mainly τ_1^{-1} but also τ_2^{-1} and I_1/I_2. As a compromise between reduced influence on, and visibility of, the 2nd exponential, the concentration of the aromatic is chosen, at any given temperature, for the adduct–to–OH ratio being about 10.

The exponential parameters with their mutual covariances are skipped by the k-fit, from which 2-σ upper limits for most of the adduct+NO reactions of 3×10^{-14} cm^3 s^{-1} are obtained at about 330 K. The uncertainty is about threefold higher in the cases of phenol, due to the higher branching ratio for its abstraction channel limiting the dynamic range of τ_2^{-1}, and p-xylene, due to the photolysis and fluorescence of the aromatic. The cycling experiments with naphthalene (Koch and Zetzsch, 1994) showed such a high yield of HO_2 that the radical loss due to adduct+NO cannot be faster than 10^{-13} cm^3 s^{-1}.

3.4 Smog chamber

Five runs with all three aromatics (benzene, toluene and p-xylene) together, two runs with benzene and one each with toluene and p-xylene were performed at OH levels ranging from 5 to 10×10^6 cm^{-3}. Figure 4 shows a run with p-xylene, where OH is produced from photolysis of H_2O_2 at 420 ppb. The logarithmic scale applies to the organics while the continuously added oxygen is plotted to the linear scale at the right. After an initial, linear increase of O_2 by 7.6 ppm/h (from very minor leaks and decomposition of H_2O_2), O_2 is increased by 35 ppm/h. The exponential consumption of the reference compounds indicates [OH] to be fairly constant while the consumption of p-xylene accelerates with [O_2]. The quantitative evaluation yields a time profile of [OH](t), reaching a stable level within less than a sampling period and slowly increasing from 8.3 to 8.6×10^6 cm^{-3} during the following 20 h.

4 Discussion

As can be seen in Table 1, the obtained adduct+NO_2-reaction rate constants are not far from collision frequency and, therefore, do not show a significant temperature dependence. On the other hand, the obtained O_2 reactivities are much lower and span a range of three orders of magnitude, with each methyl substituent increasing the reactivity by about a factor of 3 (comparing benzene with toluene, m-xylene and finally HMB). The only cases with a significant temperature dependence are the two extreme ones, benzene and HMB, with positive and negative activation energy, respectively. The factor of 3 also occurs between the adduct reactivities of phenol and m-cresol, which are, however, more reactive than the corresponding non-phenolic cases by a factor of 200. The following comparisons with literature data are sorted by scavenger species.

4.1 Reaction of the adduct with NO

For the NO reactivity of benzene–OH (hydroxycyclohexadienyl, HCHD), Zellner et al. (1985) obtained a value of 1×10^{-12} cm^3 s^{-1} which should be two orders of magnitude lower to fit within our upper limit and is probably caused by NO_2 as impurity in the NO mixture, that was used without purification. This applies as well to earlier results of Witte and Zetzsch (1988) on both, benzene–OH and toluene–OH, of 6×10^{-13} cm^3 s^{-1}, which were also not corrected for the influence of the OH+NO reaction.

4.2 Reaction of the adduct with NO_2

Zellner et al. (1985) studied also the NO_2 reaction of HCHD, fitted exponentials to absorption profiles (of the adduct and possibly subsequent products at 308.5 nm) and obtained a rate constant which is a factor of 3 below the result of this study. Goumri et al. (1990) report a value of $(4\pm2)\times10^{-11}$ cm^3 s^{-1} for toluene–OH at 297 K, and Bjergbakke et al. (1996) a value of $(1.1\pm0.2)\times10^{-11}$ cm^3 s^{-1} for HCHD at 338 K. In the latter study, the radical level was so high that almost half of the initial 0.2 mbar NO_2 were consumed and their stated observation of the peroxy radical has already been disputed (Koch, 1997).

4.3 The adduct reaction with O_2

In an additional measurement, Zellner et al. (1985) switched the bath gas (20 mbar) from N_2 to O_2 and found a slight decrease of the slope of τ_2^{-1} vs. [NO] which could be explained by cycling of OH via HO_2 from benzene oxidation. However, instead of an increased offset, τ_2^{-1} at [NO]=0, hinting at an O_2 reaction, they mention very slow decays even at 50 mbar of O_2. Based on that paper, Atkinson et al. (1989) estimated an upper limit of 2×10^{-16} cm^3 s^{-1}, just including our result. Another experiment less than a factor of 2 off the goal to detect a slow O_2 reaction is that of Perry et al. (1977), who came up with the rate constant for toluene–OH being less than or equal 1.0×10^{-15} cm^3 s^{-1}.

More recently, several authors studied the transient absorption of HCHD in the presence of O_2. Bohn and Zetzsch (1999) provided first evidence of a fast equilibrium (7/–7) in the gas phase, predicted theoretically by Lay et al. (1996) and Ghigo and Tonachini (1998) but already observed in water by Pan and Von Sonntag (1990),

$$\mathrm{HCHD} + \mathrm{O_2} \leftrightarrow \mathrm{RO_2} \qquad (7/-7)$$

by observing a decrease of the HCHD signal with O_2 and a saturation of Reaction (6), which is now explained by assuming a loss process competing with either Reaction (7) or (–7). Johnson et al. (2002) obtained an effective k_6 of 5.5×10^{-16}cm^{3}s^{-1}, considerably higher than observed in this work, 1.6×10^{-16} cm^3 s^{-1}, and by Bohn and Zetzsch (1999), 2.1×10^{-16} cm^3 s^{-1}. Improvements of the apparatus of Johnson et al. (2002) by Raoult et al. (2004) allowed the use of lower radical concentrations which resulted in slower decays, corresponding to k_6=2.5×10^{-16} cm^3 s^{-1}. These discrepancies are obviously due to radical–radical reactions. Very recently, Grebenkin and Krasnoperov (2004) obtained similarly shaped and timed decays, but proposed a radical–radical Reaction (8) instead of Reaction (6) to explain the increased loss rate with added O_2:

$$\mathrm{HCHD} + \mathrm{RO_2} \rightarrow \quad \text{products} \qquad (8)$$

Although they do not rule out Reaction (6), they denigrate it for the lack of a plausible mechanism for a reaction being both, rather slow and almost independent of temperature. Their loss mechanism, however, would lead to a strongly negative temperature dependence of the effective loss rate under our experimental conditions on the left-hand side of (7/–7), in contradiction to the slightly positive temperature dependence obtained for benzene, see Table 1.

Note also that a loss due to Reaction (8) would not saturate at high O_2 concentrations, as observed by Bohn and Zetzsch (1999), but would go through a maximum at the point where [HCHD] = [RO_2]. Although Grebenkin and Krasnoperov (2004) reach such conditions by their variation of temperature, they did not vary the O_2 concentration. They are right in stating that Reaction (6) is not needed to model their data, but this

is not a result but a limitation of their experiment: It is hard to estimate to what extent their decays, recorded not far enough into the uncertain background, are hyperbolic due to Reaction (8) or exponential due to a pseudo-first-order reaction as Reaction (6).

The parameter describing the possible influence of radical-radical reactions on the evaluation of k_6 is not the radical level itself but the radical-to-oxygen ratio. That ratio is much lower in our FP/RF experiments than in the experiments by Grebenkin and Krasnoperov (2004) and by Johnson et al. (2002) and Raoult et al. (2004) but even lower in the absorption experiments of our laboratory (Bohn and Zetzsch, 1999). In that experiment, however, an underlying background absorption with unknown formation kinetics has been subtracted, influencing the simultaneous determination of k_6 and the equilibrium constant (7/–7). The result obtained by Bohn (2001) for toluene, $(6.0\pm0.5)\times10^{-16}\,cm^3\,s^{-1}$, is in excellent agreement with this work.

4.4 Smog chamber experiments and product studies

The radical-to-oxygen ratio is difficult to estimate for our chamber experiments. In Fig. 5, the apparent rate constant for removal of the aromatic by OH, k_{app}, is plotted for all the runs of this study together with model curves calculated according to Eq. (III), where the addition channel is reduced by the back-decomposition competing with O_2,

$$k_{app} = k_2 + k_1/(1 + k_{-1}/k_6[O_2]) \quad \text{(III)}$$

using FP/RF results for adduct formation and back-decomposition and either (solid lines) reasonable values for the abstraction channel derived from our FP/RF data plus literature data at higher temperatures, or (dotted lines) the total loss observed in the FP/RF experiments exceeding reasonable values for diffusion (see Appendix).

Although the downward trend of k_{app} with decreasing O_2 follows the model curves and reaches, in the case of benzene, a fairly low value, the data is obviously less reproducible than could be expected from the accurate sample analysis. While the determination of $[O_2]$ apparently contributes to the scatter at low concentrations of O_2, this is unlikely to be significant above $10^{16}\,cm^{-3}$. The additional loss processes may

well be reactions of the adduct with peroxy radicals. While the level of OH radicals is only slightly higher than outdoors, the level of peroxy radicals may exceed the value of $10^8\,cm^{-3}$ observed in the remote boundary layer (Monks et al., 1998) by a factor of ten, since in our chamber, background NO_x is even lower. Thus, the ratio may be similar as in our FP/RF experiments, but another factor of about three should be applied to compare the steady-state concentration in the chamber with the initial concentration of the pulsed experiments. While our chamber experiments do show the drop of the apparent OH reactivity at the right range of O_2 concentrations, a heated chamber would allow experiments at higher O_2 concentrations or with more reactive adducts than benzene–OH, due to the accelerated thermal back-decomposition of the adduct.

The competition of O_2 with NO_2 takes place on an even faster time scale. While it is negligible in the tropospheric environment, it becomes important in high-NO_x chamber experiments. One can estimate the level of NO_2, $[NO_2]_{1/2}$, where half of the adducts, aromatic–OH, are scavenged by NO_2 instead of O_2. Table 2 compares the $[NO_2]_{1/2}$-levels calculated from Table 1 with values fitted to NO_2-dependent product yields of chamber experiments of Volkamer et al. (2002, yields of phenol from benzene) and Bethel et al. (2000, yields of 3-hexene-2,5-dione from p-xylene), respectively. The agreement is reasonable. Very recently, the large yield of phenol (53%) from benzene in the absence of NO_2, reported by Volkamer et al. (2002), has been confirmed by Berndt and Böge (2006), reporting 61%. The observation of a yield of 24% phenol in the presence of NO_2 at 9.6 ppm by Atkinson et al. (1989) is not too far from the expected decrease with NO_2. Furthermore, Atkinson and Aschmann (1994) reanalyzed the earlier data of Atkinson et al. (1989) on nitrobenzene from benzene +OH and m-nitrotoluene from toluene + OH as a function of NO_2 using the rate constants of Knispel et al. (1990) and found reasonable agreement of the experiment with calculated curves. In the same study, Atkinson and Aschmann (1994) observed a decrease of the yield of 2,3-butanedione from o-xylene with the expected curvature and a $[NO_2]_{1/2}$ value of about 2 ppm, confirmed by an experiment with fivefold decreased level of O_2. The decreasing yields of 2,3-butanedione from 1,2,3-trimethylbenzene and

1,2,4-trimethylbenzene with increasing NO_2 observed by Bethel et al. (2000) can be taken as a hint at a similar competition of NO_2 with O_2 in the reaction with the OH-adducts.

To conclude, the present work shows that the only relevant atmospheric scavenger for aromatic–OH adducts is O_2. While the adduct+NO reaction can be neglected even under high-NO_x simulation-chamber conditions, NO_2 levels near 1 ppm should be avoided in chamber experiments aimed at the mechanism of tropospheric aromatic oxidation.

The mechanism of the effective Reaction (6) is still unclear. It has to be either an O_2 reaction competing with Reaction (7), with phenol and HO_2 as products as calculated ab initio by Estupinan et al. (2003), or a unimolecular reaction in competition to (–7), which may be decomposition to phenol and HO_2 or an isomerisation to another intermediate. The intermediate must immediately form HO_2 (possibly in a fast reaction with a further O_2 molecule) as a high yield of prompt HO_2 is observed in our FP/RF experiments employing cycling of radicals (Koch et al., 1994 and 1997). In the tropospheric environment in the presence of NO_x, the RO_2 radical formed from Reaction (7) is known (Bohn and Zetzsch, 1999; Klotz et al., 2002) to react rapidly with NO.

Appendix A

The coefficients a, d and $b \cdot c$ can be split into three terms according to their concentration dependence:

$$a = a_0 + a_A[A] + a_S[S] \quad \text{(A1)}$$

$$b \cdot c = bc_A[A] \quad \text{(A2)}$$

$$d = d_0 + d_A[A] + d_S[S] \quad \text{(A3)}$$

To each group of biexponential decay curves (p,T=const; [A], [S] variable), a set of effective rate constants: a_0, a_A, a_S, bc_A, d_0, d_S is fitted simultaneously. Thereby $a_0=k_4$,

$a_S=k_3$ and $d_S=k_6$ result directly from the evaluation; any reaction of the adduct with the aromatic (d_A) turns out to be insignificant. The three constants $a_A=k_1+k_2$, $bc_A=k_1 k_{-1}$ and $d_0=k_{-1}+k_5$ contain four degenerate rate constants. This degeneracy can be lifted by considering the limiting cases at low and high temperature, and assuming Arrhenius behaviour for the abstraction, the addition and the unimolecular decay (k_1, k_{-1}, k_2), for the diffusion of OH (k_4) and for the diffusion of the adduct (k_5). The quantity k_5, termed adduct diffusion, includes any other thermal loss of the adduct, AOH, such as isomerisation and other reaction channels not leading back to OH. Likewise, the quantity k_2, termed abstraction, may include any impurity of the aromatics.

The coefficients b and c occur only as a product in Eq. (II) with the consequence that, by observing OH alone, there remains an uncertainty about the assignment of observed radical loss to the two sides of the equilibrium connected with a tradeoff between b and c (the product bc is determined by the data): If all the loss is due to the processes denoted Reaction (2), decreasing the contribution of c to the slope of coefficient a versus [aromatic], then c is small and b is as large as possible, $b = d$ in the absence of a scavenger. On the other hand, the loss may be assigned to processes competing with the back-decomposition of the adduct, i.e. Reaction (5) denoted adduct diffusion. In this case, the contribution of b to d decreases while c increases. Note that in the case of added scavenger, b contributes to the $offset$ of d only, while the evaluation of the target reaction ($k_6=slope$ of d) is not affected. Note also that the coefficients b and c, and thus the equilibrium constant, would only be separable if one could measure absolute concentrations of both OH and the adduct (c occurs without an accompanying factor b in the adduct–to–OH ratio).

Acknowledgements. Support of this study by the Federal Ministry for Research and Technology (grant 07 EU 705), and the Commission of the European Communities (grants STEP 0007-C and RII3-CT-2004-505968-EUROCHAMP) and the Federal Ministry of Environment is gratefully acknowledged.

References

Anastasi, C. and Smith, I. W. M.: Rate measurements of reactions of OH by resonance absorption. Part 6. – Rate constants for OH + NO(+M)→HNO_2(+M) over a wide range of temperature and pressure, J. Chem. Soc. Faraday Trans. II, 74, 1056–1064, 1978.

Atkinson, R.: Kinetics and mechanisms of the gas-phase reactions of the hydroxyl radical with organic compounds, J. Phys. Chem. Ref. Data, Monograph No. 1, 1989.

Atkinson, R.: Gas-phase tropospheric chemistry of organic compounds. A review, Atmos. Environ., 24A, 1–41, 1990.

Atkinson, R.: Gas-phase tropospheric chemistry of organic compounds, J. Phys. Chem. Ref. Data, Monograph No. 2, 1994.

Atkinson, R. and Aschmann, S. M.: Products of the gas-phase reactions of aromatic hydrocarbons: Effect of NO_2 concentration, Int. J. Chem. Kinet., 26, 929–944, 1994.

Atkinson, R. and Arey, J.: Atmospheric degradation of volatile organic compounds, Chem. Rev., 103, 4605–4638, 2003.

Atkinson, R., Aschmann, S. M., Arey, J., and Carter, W. P. L.: Formation of ring-retaining products from the OH radical-initiated reactions of benzene and toluene, Int. J. Chem. Kinet., 21, 801–827, 1989.

Behnke, W., Holländer, W., Koch, W., Nolting, F., and Zetzsch, C.: A smog chamber for studies of the photochemical degradation of chemicals in the presence of aerosols, Atmos. Environ., 22, 1113–1120, 1988.

Berndt, T. and Böge, O.: Gas-phase reaction of OH radicals with benzene: products and mechanism, Phys. Chem. Chem. Phys., 3, 4946–4956, 2001a.

Berndt, T. and Böge, O.: Rate constants for the gas-phase reaction of hexamethylbenzene with OH radicals and H atoms and of 1,3,5-trimethylbenzene with H atoms, Int. J. Chem. Kinet., 33, 124–129, 2001b.

Berndt, T. and Böge, O.: Formation of phenol and carbonyls from the reaction of OH radicals with benzene, Phys. Chem. Chem. Phys., 8, 1205–1214, 2006.

Bethel, H., Atkinson, R., and Arey, J.: Products of the gas-phase reactions of OH radicals with p-xylene and 1,2,3- and 1,2,4-trimethylbenzene: Effect of NO_2 concentration, J. Phys. Chem., A, 104, 8922–8929, 2000.

Bjergbakke, E., Sillesen, A., and Pagsberg, P.: UV spectrum and kinetics of hydroxycyclohexadienyl radicals, J. Phys. Chem., 5729–5736, 1996, Comment by Koch, R., J. Phys. Chem. B,

101, 293, 1997.

Bloss, C., Wagner, V., Bonzanini, A., Jenkin, M. E., Wirtz, K., Martin-Reviejo, M., and Pilling, M. J.: Evaluation of detailed aromatic mechanisms (MCMv3 and MCMv3.1) against environmental chamber data, Atmos. Chem. Phys. Discuss., 4, 5683–5731, 2004, Interactive comment by Referee #2, ibid., S2391–2395, 2004.

Bohn, B.: Formation of peroxy radicals from OH–toluene adducts and O_2, J. Phys. Chem. A, 105, 6092–6101, 2001.

Bohn, B. and Zetzsch, C.: Gas-phase reaction of the OH–benzene adduct with O_2: Reversibility and secondary formation of HO_2, Phys. Chem. Chem. Phys., 1, 5097–5107, 1999.

Calvert, J. G., Atkinson, R., Becker, K. H., Kamens, R. M., Seinfeld, J. H., Wallington, T. H., and Yarwood, G.: The mechanisms of atmospheric oxidation of aromatic hydrocarbons, Oxford Univ. Press, 2002.

Elend, M. and Zetzsch, C.: The influence of oxygen on the apparent rate constant for the reaction of OH with aromatics in smog chamber experiments in nitrogen at one atmosphere, in: Laboratory studies on atmospheric chemistry, air pollution research report 42 (Proc. CEC/EUROTRAC workshop, York 1991), CEC, Brussels, 123–126, 1992.

Estupinan, E., Villenave, E., Raoult, S., Rayez, J. C., Rayez, M. T., and Lesclaux, R.: Kinetics and mechanism of the gas-phase reaction of the cyclohexadienyl radical c-C_6H_7 with O_2, Phys. Chem. Chem. Phys., 5, 4840–4845, 2003.

Ghigo, G. and Tonachini, G.: Benzene oxidation in the troposphere: theoretical investigation of the possible competition of three postulated reaction channels, J. Amer. Chem. Soc. 120, 6753–6757, 1998.

Goumri, A., Sawerysyn, J.-P., Pauwels, J.-F., and Devolder P.: Tropospheric oxidation of toluene: Reactions of some intermediate radicals, in: Physico-chemical behaviour of atmospheric pollutants, edited by: Restelli, G. and Angeletti, G., Kluwer Acad. Publ., Dordrecht, 315–319, 1990.

Grebenkin, S. Y. and Krasnoperov, L. N.: Kinetics and thermochemistry of the hydroxycyclohexadienyl radical reaction with O_2: $C_6H_6OH + O_2 \rightarrow C_6H_6(OH)OO$, J. Phys. Chem. A, 108, 1953–1963, 2004.

Jenkin, M. E., Saunders, S. M., Wagner, V., and Pilling, M. J.: Protocol for the development of the Master Chemical Mechanism, MCM v3 (Part B): Tropospheric degradation of aromatic volatile organic compounds, Atmos. Chem. Phys., 3, 181–193, 2003.

Johnson, D., Raoult, S. , Rayez, M.-T., Rayez, J.-C., and Lesclaux, R.: An experimental and

theoretical investigation of the gas-phase benzene–OH radical adduct + O_2 reaction, Phys. Chem. Chem. Phys., 4, 4678–4686, 2002.

Johnson, D., Raoult, S., Lesclaux, R., and Krasnoperov, L.N.: UV absorption spectra of methyl-substituted hydroxy-cyclohexdienyl radicals in the gas phase, J. Photochem. Photobiol. A, 176, 98–106, 2005.

Klotz, B., Volkamer, R., Hurley, M. D., Sulbaeck Andersen, M. P., Nielsen, O.J., Barnes, I., Imamura, T., Wirtz, K., Becker, K. H., Platt, U., Wallington, T. J., and Washida, N.: OH-initiated oxidation of benzene, Part II. Influence of elevated NO_x concentrations, Phys. Chem. Chem. Phys., 4, 4399–4411, 2002.

Knispel, R., Koch, R., Siese, M., and Zetzsch, C.: Adduct formation of OH radicals with benzene, toluene, and phenol and consecutive reactions of the adducts with NO_x and O_2, Ber. Bunsenges. Phys. Chem., 94, 1375–1379, 1990.

Koch, R.: Kinetische Untersuchung der Folgereaktionen der OH-Addukte mit NO, NO_2 und O_2 mit simultaner Auswertung von Kurvenscharen, PhD thesis, Univ. of Hannover, 1992.

Koch, R., Bohn, B., and Zetzsch, C.: Cycles of HO_x as a tool to investigate the tropospheric chemistry of aromatics in kinetic experiments, in: The oxidizing capacity of the troposphere, physico-chemical behaviour of atmospheric pollutants, edited by: Larsen, B., Versino, B., and Angeletti, G., European Commission, Brussels, 217–221, 1997.

Koch, R., Knispel, R., Siese, M., and Zetzsch, C.: Absolute rate constants and products of secondary steps in the atmospheric degradation of aromatics, in: Physico-chemical behaviour of atmospheric pollutants, edited by: Angeletti, G. and Restelli, G., European Commission, Brussels/Luxemburg, 143–149, 1994.

Koch, R. and Zetzsch, C.: Cycling of OH radicals in the system naphthalene/O_2/NO studied by FP/RF and LP/RF, presented at the 13th Int. Sympos. on Gas Kinetics, Dublin, 1994.

Lay, T. H., Bozzelli, J. W., and Seinfeld, J. H.: Atmospheric photochemical oxidation of benzene: Benzene + OH and the benzene–OH adduct (hydroxyl-2,4-cyclohexadienyl) + O_2, J. Phys. Chem., 100, 6543–6554, 1996.

Michael, J. V., Nava, D. F., Payne, W. A., Lee, J. H., and Stief, L. J.: Rate constant for the reaction atomic hydrogen + nitrogen dioxide from 195 to 400 K with FP-RF and DF-RF techniques, J. Phys. Chem., 83, 2818–2823, 1979.

Monks, P. S., Carpenter, L. J., Penkett, S. A., Ayers, G. P., Gillett, R. W., Galbally, I. E., and Meyer, C. P. (Mick): Fundamental ozone photochemistry in the remote marine boundary layer: The SOAPEX experiment, measurement and theory, Atmos. Environ., 32, 3647–3664,

1998.

Nolting, F., Behnke, W., and Zetzsch, C.: A smog chamber for studies of the reactions of terpenes and alkanes with ozone and OH, J. Atmos. Chem., 6, 47–59, 1988.

Pan, X. M. and von Sonntag, C.: Hydroxyl-radical-induced oxidation of benzene in the presence of oxygen: $R\cdot + O_2 \leftrightarrow RO_2\cdot$ equilibria in aqueous solution. A pulse radiolysis study, Zeitschrift fuer Naturforschung, B: Chemical Sciences, 45, 1337–1340, 1990.

Paraskevopoulos, G. and Singleton, D. L.: Reactions of OH radicals with inorganic compounds in the gas phase, Rev. Chem. Intermed., 10, 139–218, 1988.

Perry, R. A., Atkinson, R., and Pitts, Jr. J. N.: Kinetics and mechanism of the gas phase reaction of OH radicals with aromatic hydrocarbons over the temperature range 296–473 K, J. Phys. Chem., 81, 296–304, 1977.

Press, W. H., Teukolsky, S. A., Vetterling, W. T., and Flannery, B. P.: Numerical recipes in FORTRAN: The Art of Scientific Computing, Cambridge Univ. Press, 1992.

Raoult, S., Rayez, M.-T., Rayez, J.-C., and Lesclaux, R.: Gas-phase oxidation of benzene: Kinetics, thermochemistry and mechanism of initial steps, Phys. Chem. Chem. Phys., 6, 2245–2253, 2004.

Rinke, M. and Zetzsch, C. : Rate constants for the reactions of OH-radicals with aromatics: benzene, phenol. aniline and 1,2,4-trichlorobenzene, Ber. Bunsenges. Phys. Chem., 88, 55–62, 1984.

Stuhl, F. and Niki, H.: Flash photochemical study of the reaction OH+NO+M using resonance fluorescent detection of OH, J. Chem. Phys., 57, 3677–3679, 1972.

Volkamer, R., Klotz, B., Barnes, I., Imamura, T., Wirtz, K., Washida, N., Becker, K. H., and Platt, U.: OH-initiated oxidation of benzene, Part I. Phenol formation under atmospheric conditions, Phys. Chem. Chem. Phys., 4, 1598–1610, 2002.

Wagner, H. G., Welzbacher, U., and Zellner, R.: Rate measurements for the reactions H + $NO_2 \rightarrow$ OH + NO and H + NOCl $\rightarrow$ HCl + NO by Lyman-alpha fluorescence, Ber. Bunsenges. Phys. Chem., 80, 1023–1027, 1976.

Wahner, A. and Zetzsch, C.: Rate constants for the addition of OH to aromatics (benzene, p-chloroaniline and o-, m- and p-dichlorobenzene) and the unimolecular decay of the adduct. Kinetics into a quasi-equilibrium, J. Phys. Chem., 87, 4945–4951, 1983.

Wallington, T. J., Neuman, D. M., and Kurylo, M. J.: Kinetics of the gas phase reaction of hydroxyl radicals with ethane, benzene and a series of halogenated benzenes over the temperature range 234–438 K, Int. J. Chem. Kinet., 19, 725–739, 1987.

Witte, F., Urbanik, E., and Zetzsch, C.: Temperature dependence of the rate constants for the addition of OH to benzene and to some monosubstituted aromatics (aniline, bromobenzene and nitrobenzene) and the unimolecular decay of the adducts. Kinetics into a quasi-equilibrium 2, J. Phys. Chem., 90, 3251–3259, 1986.

Witte, F. and Zetzsch, C.: Annual report of the steering committee of LACTOZ, a joint EUROTRAC/COST 611 project, EUREKA/CEC, Brussels, 62–66, 1988.

Zellner, R., Fritz, B., and Preidel, M.: A cw UV laser absorption study of the reactions of the hydroxy-cyclohexadienyl radical with NO_2 and NO, Chem. Phys. Lett., 121, 412–416, 1985.

Zetzsch, C., Koch, R., Siese, M., Witte, F., and Devolder, P.: Adduct formation of OH with benzene and toluene and reaction of the adducts with NO and NO_2, in: Physico-Chemical Behaviour of Atmospheric Pollutants, edited by: Restelli, G. and Angeletti, G., Kluwer Acad. Publ., Dordrecht, 320–327, 1990.

Zetzsch, C., Koch, R., Bohn, B., Knispel, R., Siese, M., and Witte, F.: Adduct formation of OH with aromatics and unsaturated hydrocarbons and consecutive reactions with O_2 and NO_x to regenerate OH, in: Chemical Processes in Atmospheric Oxidation, edited by: Le Bras, G., Springer, Berlin, 1997, 247–256.

Table 1. Rate constants for reactions of adducts, aromatic–OH, with O_2 and NO_2 obtained by FP/RF at various temperatures (T in K), employing flash photolysis of H_2O at 130 mbar in Ar.

k ($cm^3\ s^{-1}$)	Benzene[a]	Toluene[a]	m-Xylene[c]	p-Xylene	HMB[d]	Aniline	Phenol[a]	m-Cresol
$k^{add}_{O2}/10^{-16}$	1.6±0.6[b] (299)	5.6±1.5[b] (299)	18±5 (303)	8.8±2.5 (298)		6±2 (320)	300±70 (323)	640±150 (317)
	2.1±0.4[b] (314)	5.6±0.6[b] (321)	16±3 (323)	8.3±2.0 (308)		15±5 (340)	260±60 (333)	750±150 (319)
	3.0±0.3[b] (333)	5.6±0.6 (339)		8.7±1.5 (319)	1800±300 (355)	9.6±3 (350)	270±50[e] (337)	> 800 (324)
	3.7±0.4[b] (354)	5.3±0.7 (347)		7.1±1.0 (327)			290±60 (343)	820±100 (334)
		5.9±0.8 (354)		8.8±1.5 (332)	1200±200 (385)		270±60 (353)	800±100 (350)
							360±50[e](363)	
$k^{add}_{NO2}/10^{-11}$	2.75±0.4 (305)	3.6±0.5 (300)		3.5±0.5 (317)		5±2 (330)	3.4±0.6[b] (331)	4±1 (317)
	2.45±0.3 (320)	3.6±0.4 (311)		2.9±0.5 (330)			4.1±0.7[b] (354)	4±1 (325)
	2.5±0.4 (333)	3.6±0.4 (320)						
	2.5±0.4 (349)	4.0±0.6 (338)						

[a]Published before (Knispel et al., 1990),
[b]re-evaluated (Koch, 1992),
[c]laser photolysis of N_2O in He,
[d]250 mbar of He,
[e]30 to 300 mbar Ar.

Table 2. Scavenging by NO_2 calculated from FP/RF data and observed in smog chambers for the OH-adducts of benzene, toluene and p-xylene.

Aromatic	$[NO_2]_{1/2}$(ppm)		
	FP/RF	Chamber	
Benzene	1.3	~2[a]	Volkamer et al. (2002)
Toluene	3.3	[a]	
p-Xylene	5.1	4.3	Bethel et al. (2000)

[a]See also discussion by Atkinson and Aschmann 1994.

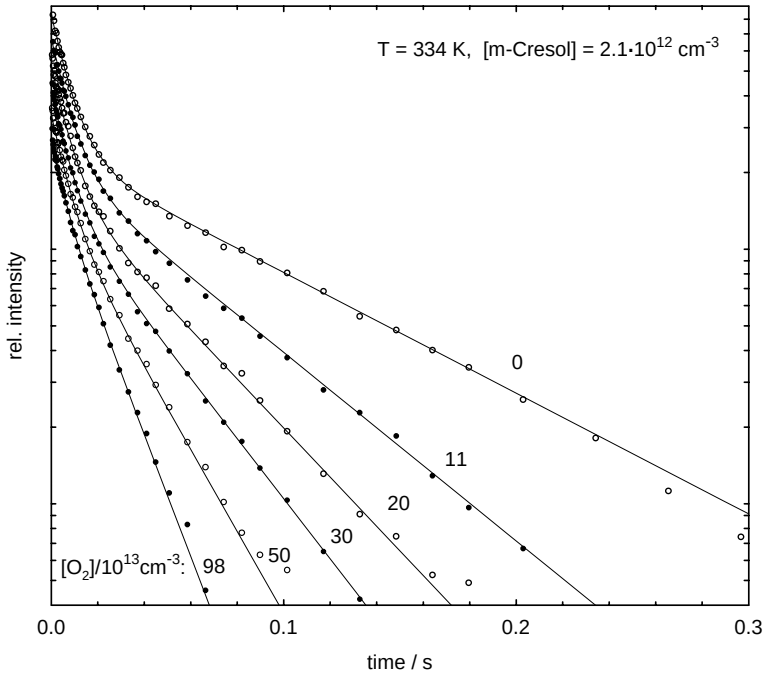

Fig. 1. Biexponential decays of OH in the presence of m-cresol and O_2 in 127 mbar of Ar at 334 K. The curves represent the result of a fit of the title reaction to 12 OH decays (these 6 and 6 similar ones), where the parameters describing the O_2-free system are fixed to values determined from another set of decays with and without m-cresol.

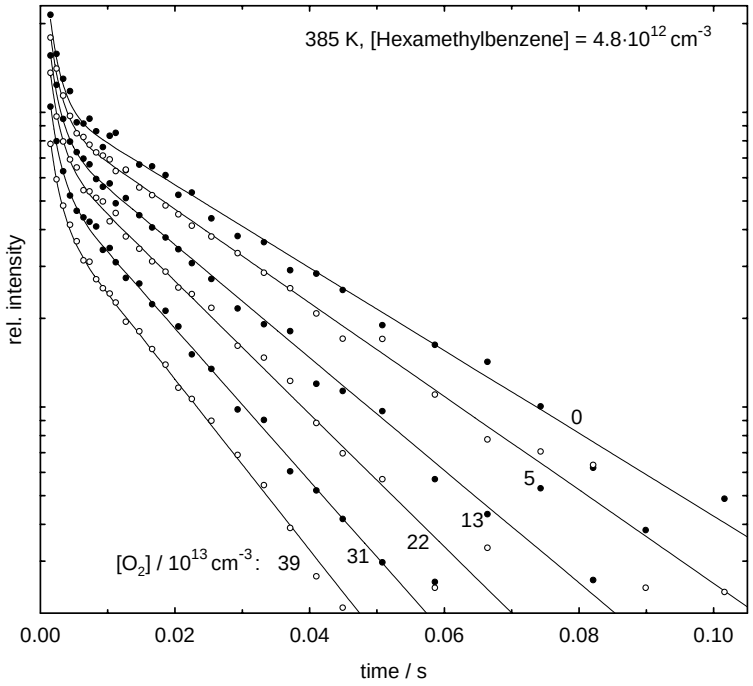

Fig. 2. Biexponential decays of OH in the presence of HMB and O_2 in 250 mbar of He at 385 K. The curves represent the result of a fit of the title reaction to 10 OH decays (these 6 and 4 similar ones at [HMB] = 1.0×10^{12} cm^{-3}).

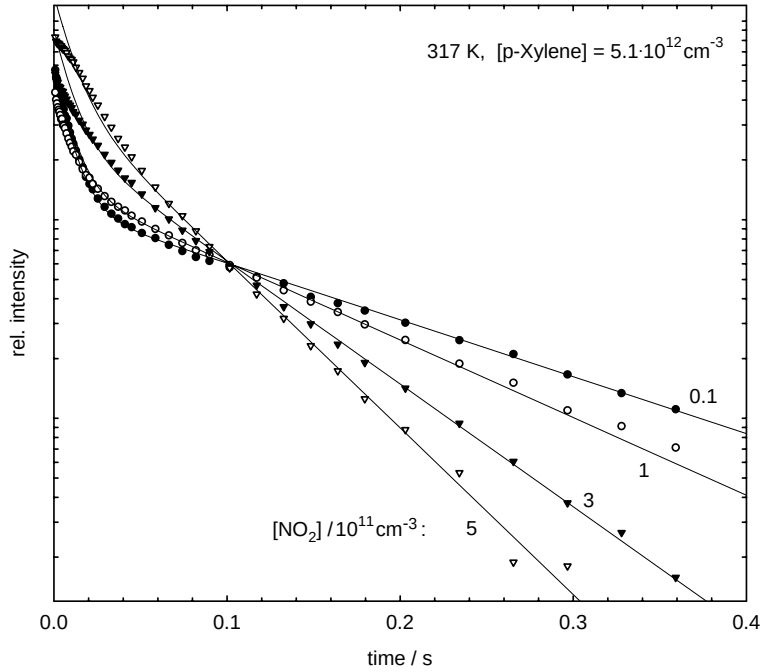

Fig. 3. Triexponential decays of OH in the presence of p-xylene (5×10^{12} cm^{-3}) and NO_2 in 130 mbar of Ar at 317 K. The triexponential model curves represent the result of a global fit. Obviously, the [NO_2]-dependence of the final slopes is well described by the model while the earlier parts of the decays had to be excluded from the fit (see text).

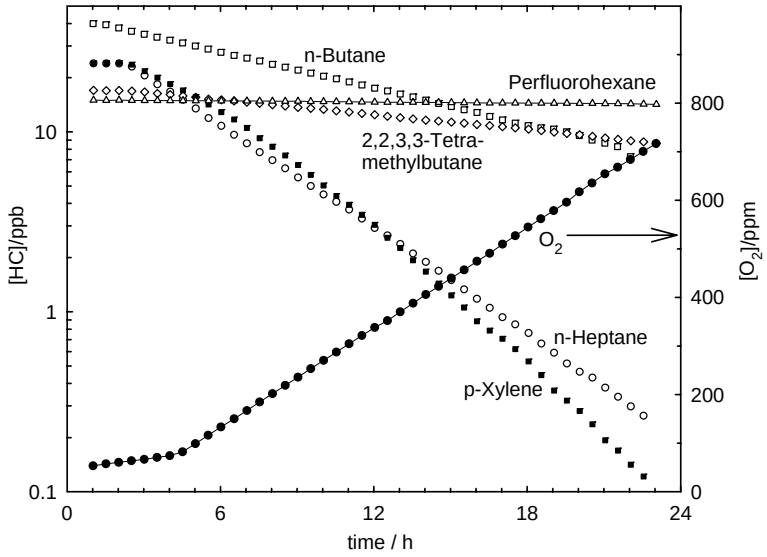

Fig. 4. Chamber experiment on p-xylene. Dilution-corrected time profiles of the organic compounds (to the logarithmic ppb scale) and [O_2] (linear ppm scale). Lights were switched on at t=2.4 h, and continuous addition of O_2 starts at 4.5 h. Note the curvature observed for p-xylene, indicating an O_2-dependent rate constant, in contrast to the alkanes.

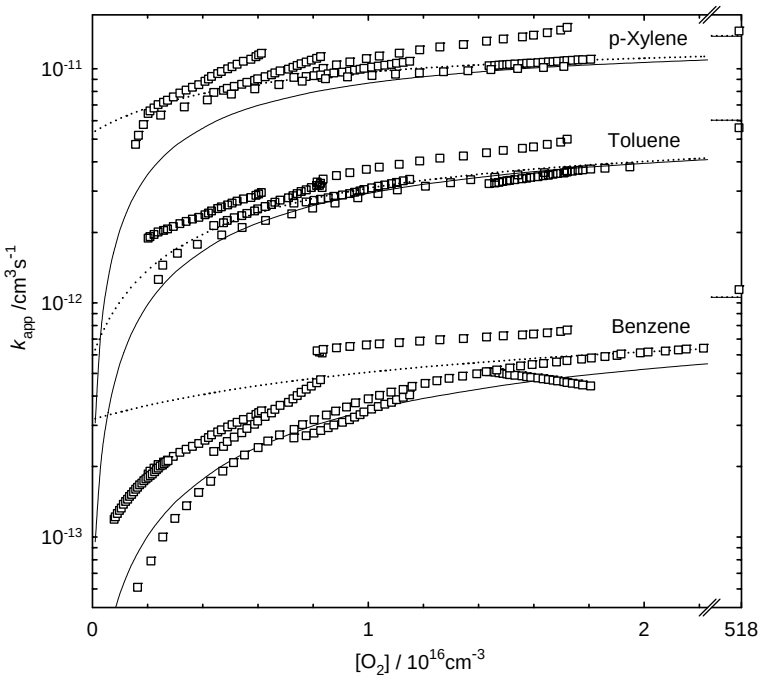

Fig. 5. Rate constants for the removal of aromatics by OH in nitrogen as a function of [O2] up to atmospheric composition, 300 K, 1 bar. Model curves are calculated according to Eq. (III) using rate constants obtained with FP/RF (see text).